RESEARCH ARTICLE
doi: 10.2306/scienceasia1513-1874.2010.36.231

ScienceAsia 36 (2010): **231–236**

Structural and electrical properties of $(1-x)\,Na_{0.465}K_{0.465}Li_{0.07}Nb_{0.93}Ta_{0.07}O_3$–$x$ MnO lead-free piezoelectric ceramics synthesized at low sintering temperatures

Pornsuda Bomlai[a,d,*], **Chanoknate Songsurin**[a], **Nantakan Muensit**[b,d], **Steven J. Milne**[c]

[a] Department of Materials Science and Technology, Faculty of Science, Prince of Songkla University, Songkhla 90112 Thailand
[b] Department of Physics, Faculty of Science, Prince of Songkla University, Songkhla 90112 Thailand
[c] Institute for Materials Research, University of Leeds, Leeds LS2 9JT, UK
[d] NANOTEC Centre of Excellence at Prince of Songkla University, Thailand

*Corresponding author, e-mail: ppornsuda@yahoo.com

Received 24 Mar 2010
Accepted 20 Jun 2010

ABSTRACT: Ceramics of the lead-free piezoelectric ceramic composition, $Na_{0.465}K_{0.465}Li_{0.07}Nb_{0.93}Ta_{0.07}O_3$, (NKLNT), were prepared using a reaction sintering method. The effects of manganese oxide doping on the structural and electrical properties of NKLNT ceramics were investigated. Variations in the relative intensity of X-ray diffraction peaks were consistent with Mn ions substituting on the perovskite lattice to produce a change in the proportions of co-existing tetragonal and orthorhombic phases. Grain growth during secondary recrystallization was also affected, leading to more uniform microstructures. The temperature of the orthorhombic-tetragonal (O-T) phase transition decreased, and the Curie temperature increased as a result of Mn modifications. The dielectric dissipation factors were lowered by Mn incorporation, but the d_{33} piezoelectric charge coefficient fell from 190 pC/N to $\leqslant$ 144 pC/N due to the shift in the O-T phase transition to well below room-temperature.

KEYWORDS: doping, phase formation, microstructure, dielectric and piezoelectric properties

INTRODUCTION

Lead zirconate titanate (PZT) based piezoelectric ceramics have been widely used in the manufacture of actuators, sensors, transducers, and other devices in recent years [1–3]. Because of the detrimental effects of Pb on human health, it is important that Pb-free ferroelectric and piezoelectric materials are developed. The new environmentally acceptable and biocompatible materials should exhibit electrical properties comparable to those of Pb-based ferroelectrics which have been developed over several decades.

Currently, sodium potassium niobate, $(Na_{0.5}K_{0.5})NbO_3$ (NKN) based ceramics are one of the most promising alternative systems to PZT because of their excellent piezoelectric properties, high Curie temperature, and low environmental impact [4–6]. Research into these materials increased after Saito et al [7] reported textured (Li, Sb, Ta) modified NKN ceramics with comparable piezoelectric properties (d_{33} = 416 pC/N, k_p = 61%) to a hard PZT. However, it is well known that dense and well sintered NKN ceramics are very difficult to obtain by ordinary sintering processes because of the high volatility of alkali metal oxides at high temperatures. Therefore, many studies have been carried out to improve the densification and electrical properties of NKN ceramics, such as the formation of solid solutions with other oxides, e.g., NKN–$BaTiO_3$ [8], NKN–$LiNbO_3$ [9], NKN–$LiSbO_3$ [10], NKN–$LiTaO_3$ [11,12], NKN–$LiTaO_3$–$LiSbO_3$ [7,13]. The effects of sintering aids such as CuO [14], ZnO [15], and Bi_2O_3 have also been studied [16].

Although it was previously reported that the highest d_{33} coefficients in the binary NKN–LT system are obtained at 5–6 mol% $LiTaO_3$, Skidmore et al [17] showed that the NKN–7 mol% $LiTaO_3$ composition, $[Na_{0.5}K_{0.5}NbO_3]_{0.93}$–$[LiTaO_3]_{0.07}$, offers more favourable temperature stability of dielectric and piezoelectric properties than the 5–6% $LiTaO_3$ ceramics. Moreover, the d_{33} value for NKN–7 mol% $LiTaO_3$, $\sim$ 200 pC/N, is similar to that of the 5–6 mol% $LiTaO_3$ compositions. It has been reported

that MnO/MnO_2 additions improve the densification and electrical properties of other NKN-based ceramics[18–21]. The multivalent additive suppresses grain growth and helps to increase the electrical resistivity of the piezoceramic. In this work, the effects of incorporating manganese oxide to $[Na_{0.5}K_{0.5}NbO_3]_{0.93}$–$[LiTaO_3]_{0.07}$ (abbreviated as NKLNT) are investigated.

MATERIALS AND METHODS

Sample compositions, $(1-x)\,Na_{0.465}\,K_{0.465}\,Li_{0.07}\,Nb_{0.93}\,Ta_{0.07}O_3$–$x$ MnO with $x = 0$, 0.005, and 0.01 (i.e., 0, 0.5, and 1.0 mol% MnO), were prepared by the conventional mixed oxide process using Na_2CO_3 (Sigma-Aldrich, 99.8–100% purity), K_2CO_3, Ta_2O_5 (Sigma-Aldrich, 99% purity), Nb_2O_5, $MnCO_3$ (Sigma-Aldrich, 99.9% purity), and Li_2CO_3 (Fluka, $>$ 99.0% purity), as the starting powders. A $Na_{0.5}K_{0.5}NbO_3$ powder was prepared before reacting with Li, Ta, and Mn reagents. The carbonate powders are moisture-sensitive; niobium and tantalum oxides can also form hydrated phases. Hence, to avoid compositional errors when weighing out the precursor mixture, the starting reagents were dried in an oven for 24 h before use. Dried powders were allowed to cool to room temperature under reduced pressure in a desiccator; all powders were stored in the desiccator until immediately prior to weighing in the correct proportions. The starting materials were transferred to a 100 mm diameter cylindrical plastic jar, partially filled with 10 mm diameter zirconia grinding balls. Sufficient ethanol was added to cover the powder/media. Ball milling was carried out for 24 h, followed by drying at 120 °C. An alumina mortar and pestle was used to break up large agglomerates formed during drying. The mixtures were calcined in alumina crucibles with loosely fitting lids at 800 °C for 2 h. The NKN powders were then ground, weighed, and ball milled again for 24 h with Ta_2O_5, Li_2CO_3, and $MnCO_3$ to obtain compositions $(1-x)\,Na_{0.465}\,K_{0.465}\,Li_{0.07}\,Nb_{0.93}\,Ta_{0.07}O_3$–$x$ MnO, for 0, 0.5, and 1.0 mol% MnO modifications ($x = 0$, 0.005, 0.01). A reaction-sintering approach was used to produce the NKLNT and MnO-modified ceramics, in that no second powder calcination step was employed. The combined powders were dried, ground, and pressed at 150 MPa for 3 min into 1.5 cm diameter disks, placed in alumina crucibles, and sintered at temperatures ranging from 1025 °C to 1075 °C for 2 h in closed crucibles. Pellets were embedded in a NKLNT 'atmosphere' powder during sintering.

Ceramic samples were examined at room temperature using X-ray powder diffraction (XRD; Philips X' Pert MPD, Ni-filtered CuK_α radiation) to identify the phases formed. Sintered pellet densities were obtained by the Archimedes method. The microstructures of the as-sintered surfaces of the samples were imaged directly, using scanning electron microscopy (JEOL, Tokyo, JSM-5800LV). In order to investigate dielectric and piezoelectric properties, pellets were electroded with silver paste. The capacitance and dissipation factor (D) of the samples were measured at 1 kHz using an LCR meter (GW Instek; LCR 821) over the temperature range 25–500 °C, from which the dielectric constant (ε_r) was calculated. For piezoelectric property measurements, the samples were polarized under a DC field of 3 kV/mm at 160 °C in a silicone oil bath for 30 min. The piezoelectric coefficient (d_{33}) was then measured using a piezo-d_{33} meter (APC International; YE2730A).

RESULTS AND DISCUSSION

Fig. 1 shows the XRD patterns of $(1-x)$ NKLNT–x MnO samples which had been sintered at 1025 °C for 2 h. The intensity ratio of the pair of peaks at $2\theta = 45$–$46.5°$ in each pattern was used as an indication of the tetragonal/orthorhombic phase content[22]. The lower angle peak in the pair corresponds to the (220) peak of an orthorhombic NKN–LT phase, or the (002) peak of the tetragonal phase of NKN–LT[23,24]. The neighbouring higher angle peak corresponds to the orthorhombic (002) peak, or the (200) peak of tetragonal NKN–LT. If the sample were single-phase tetragonal NKN–LT, from previous reports the intensity ratio of this pair of peaks (I_{200}/I_{002}) is expected to be $\sim$ 2. If the sample were single phase orthorhombic, the corresponding ratio (intensity of higher angle peak)/(intensity of lower angle peak), is expected to be $\sim$ 0.5[22]. Hence a mixture of

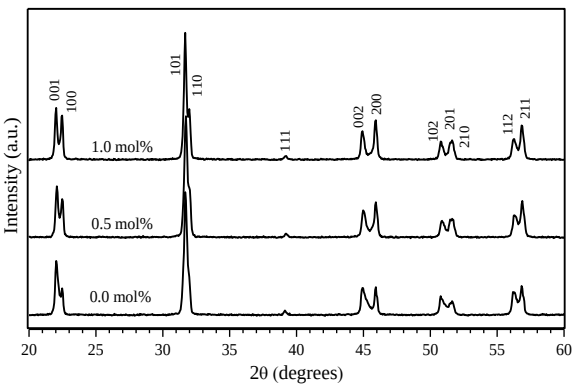

Fig. 1 XRD patterns of $(1-x)$ NKLNT–x MnO ceramics sintered at 1025 °C.

orthorhombic and tetragonal phases is expected from a measured intensity ratio of $\sim$ 1.0, determined here for the 2θ = 45–46.5° peaks in the XRD pattern of the sample of unmodified NKN–7 mol% LT sintered at 1025 °C. However Skidmore et al[22] found this composition to be tetragonal at room-temperature; variations in process conditions may have resulted in differing amounts of volatilization of Na, K, and Li oxides. Deviations in composition arising from loss of alkali metal oxides is known to alter the position of the orthorhombic-tetragonal phase transition in NKN–LT[22]. The phases present at room-temperature in this region of the NKN–LT phase diagram will therefore be dependent on the extent of volatilization losses.

The XRD peak ratio values were higher for the MnO modified samples. The sample modified with 0.5 mol% MnO gave a value of 1.2. For the 1 mol% MnO sample the peak ratio was 1.4. The higher values of peak intensity ratio of both of the MnO-modified samples suggest that the proportion of tetragonal phase increases on incorporating MnO, but there continues to be a mixture of tetragonal and orthorhombic phases present in all samples.

It has been reported previously that MnO acts as a sintering aid in the related NKN-based system, $(Na_{1-x}K_x)(Nb_{1-y}Sb_y)O_3$, but it was thought that MnO did not affect the crystal structure significantly[19]. By contrast the present XRD data for the NKLNT composition, shows that the dopant induces a change in tetragonal/orthorhombic phase content, indicating that the Mn^{2+}/Mn^{3+} ions have substituted on the perovskite lattice. The dopant may promote the stability of the tetragonal phase in the NKN–7%LT parent composition through a slight change in the position of the tetragonal-orthorhombic phase boundary on the NKN–LT phase diagram[11,12].

The highest density samples were produced at a sintering temperature of 1025 °C. For unmodified NKLNT (0% MnO), the density was 4.21 ± 0.01 g/cm^3, increasing slightly to 4.25 ± 0.05 g/cm^3 for 0.5 and 1 mol% MnO samples. Increasing the sintering temperature from 1025 °C to 1050 °C led to a significant decrease in pellet density. Density values were $\sim$ 4.0 g/cm^3 for the 0 and 0.5 mol% MnO samples and $\sim$ 3.9 g/cm^3 for the 1 mol% MnO sample sintered at 1050 °C. Density values for samples sintered at 1075 °C were generally similar to the 1050 °C samples (Fig. 2). This result indicates that of the three temperatures studied, the highest pellet density was obtained by sintering at 1025 °C; there was only a slight enhancement in density for MnO additions. The decrease in sintered density between 1050 °C and 1075 °C is most probably due to the effects of loss of volatile oxides, but partial melting is a further possibility. Based on the value of the theoretical density for NKN–7mol% LT calculated from lattice parameter measurements[17,22] the maximum relative density of the samples was around 90%.

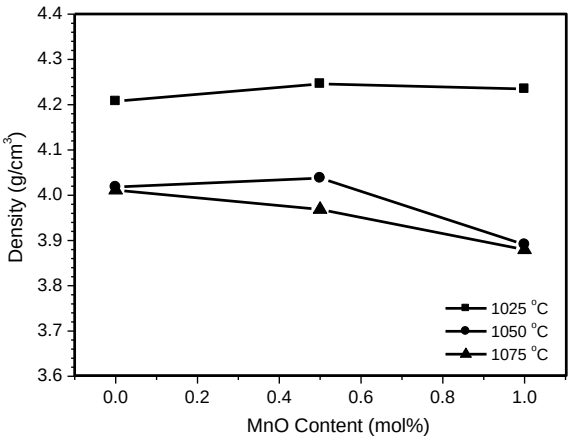

Fig. 2 Density values of $(1-x)$ NKLNT–x MnO when reaction-sintered at different temperatures.

The microstructures of samples sintered at 1025 °C showed that the grain size and morphology were also sensitive to MnO content. For the $x = 0$ composition, the structure was typical of secondary recrystallization (secondary grain growth), with a bimodal grain size composed of large grains up to $\sim$ 10–15 μm in size, co-existing with $\sim$ 1 μm grains (Fig. 3a). Incorporation of MnO led to more advanced secondary grain growth at 1025 °C, resulting in a greater proportion of the large (secondary) grain fraction, and a narrower range of grain sizes (Fig. 3b and c).

In other perovskites such as $BaTiO_3$, secondary grain growth is often associated with liquid phase formation. A similar mechanism leading to bimodal grain size distributions is probable in the $(1-x)$ NKLNT–x MnO system. However, MnO acts as a grain growth inhibitor in the perovskite $BaTiO_3$ and (Ba,Sr)TiO_3 systems. In NKLNT, it is demonstrated here to have the reverse effect, promoting secondary recrystallization such that no primary $\sim$ 1 μm grains were evident after sintering at 1025 °C for 2 h. This contrasts to the unmodified NKLNT sample which showed an intermediate stage in secondary grain growth, with primary grains coexisting with larger grains. The underlying reasons for the changes in microstructure induced by MnO are uncertain, but the additive may alter the amount of liquid present during

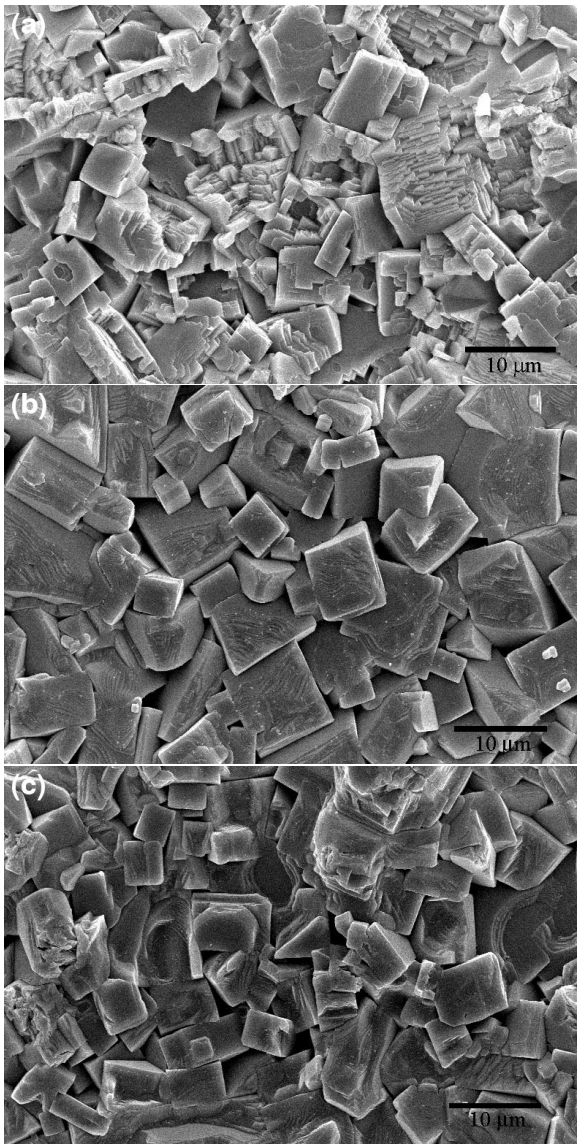

Fig. 3 SEM micrographs $(1-x)$ NKLNT–x MnO samples where x corresponds to: (a) 0 mol%, (b) 0.5 mol%, and (c) 1.0 mol% sintered at 1025 °C for 2 h.

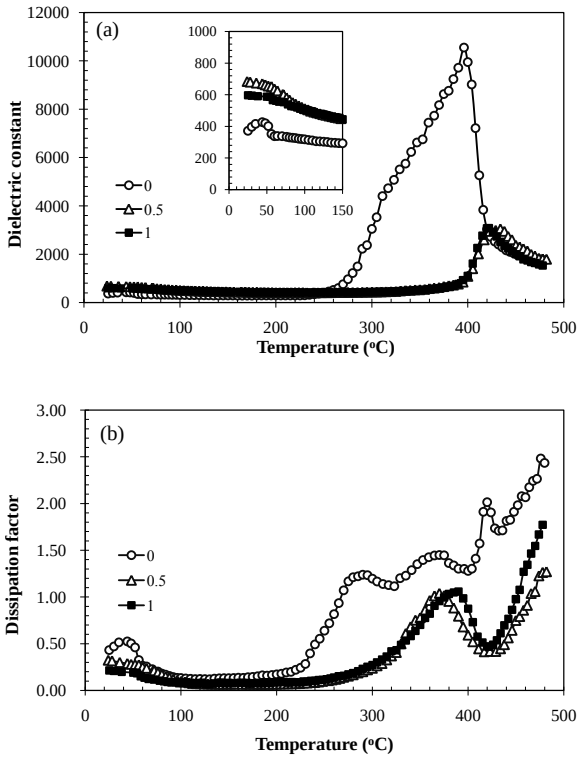

Fig. 4 Dielectric constant (measured at 1 kHz) of $(1-x)$ NKLNT–x MnO samples when sintered at 1025 °C for 2 h: (a) dielectric constant (b) dissipation factor.

sintering. Changes in defect chemistry due to lattice substitutions may also contribute to variations in mass transport and grain growth.

Measurements of dielectric constant as a function of temperature provided further information on the phase transitions in NKLNT. The values of dielectric constant (at 1 kHz) as a function of MnO content for samples sintered at 1025 °C are shown in Fig. 4a. The unmodified NKLNT sample showed a low-temperature broad dielectric peak due to an orthorhombic-tetragonal transition temperature ($T_{\mathrm{T-O}}$), or possibly a monoclinic-tetragonal[16] polymorphic phase transition, with a peak temperature at $\sim$ 45 °C (Fig. 4a, inset). A dielectric peak at higher temperatures, $\sim$ 396 °C, corresponded to the tetragonal-cubic ferroelectric phase transition. Shouldering on the low temperature side of this Curie peak may be a result of chemical inhomogeneity associated with the reaction-sintering fabrication process. Regions of different composition would give slightly different Curie temperatures (T_{C}). Overlap of Curie peaks from regions of different composition could result in a single, broad peak as observed in Fig. 4. After modification with MnO, the Curie peak became much sharper, consistent with improved chemical homogeneity. The T_{C} value increased to $\sim$ 434 °C for 0.5 mol% MnO, and 422 °C for 1 mol% MnO. The height of the dielectric peak reduced from $\varepsilon_{\mathrm{r,max}} \sim$ 11 000 to $\sim$ 3000 in the MnO-doped samples.

For the 0.5 mol% and 1 mol% MnO samples, no dielectric peaks were evident at low-temperatures (minimum measurement temperature = 25 °C). The plots did however show a slight decrease in dielectric constant as temperatures increased from 25–50 °C which could signify the tail of a O-T transition which

Table 1 The orthorhombic-tetragonal polymorphic phase transition temperature (T_{O-T}), Curie temperature (T_C) and piezoelectric (d_{33}) constant of $(1-x)$ NKLNT–x MnO samples when sintered at 1025 °C for 2 h.

MnO Content (mol%)	T_{O-T} (°C)	T_C (°C)	d_{33} (pC/N)
0.0	44	396	190
0.5	–	434	144
1.0	–	422	135

peaks at temperatures $<$ 25 °C, but cryogenic measurements would be required to explore this further.

The value of dissipation factor was lowered by the incorporation of MnO dopant. The presence of a dielectric transition at $\sim$ 45 °C in the undoped sample (Fig. 4a) complicated the comparison of room-temperature dissipation factors between the three samples (Fig. 4b). Multiple sub-peaks in the dissipation factor of unmodified NKLNT around the Curie temperature were consistent with the premise of local fluctuations in composition. All samples showed a minimum dissipation factor in the temperature range between the two dielectric transitions. At temperatures between 100–200 °C, the value fell from 0.17 for the unmodified sample to $\sim$ 0.06 for the MnO doped samples. At temperatures above the Curie temperature the dissipation factors increased rapidly, owing to conductive losses (Fig. 4b).

The values of d_{33} piezoelectric charge coefficient are shown in Table 1. In general, favourable piezoelectric coefficients for $BaTiO_3$ and other perovskite materials result when phases co-exist at a phase boundary. The highest piezoelectric coefficient at room temperature, d_{33} = 190 pC/N, was achieved in the unmodified sample for which a broad phase transition occurred with a peak-temperature of $\sim$ 45 °C. Dielectric measurements on NKLNT were carried out at $\sim$ 30 °C and therefore the adjacent polymorphic phase transition is expected to contribute to an enhancement in the d_{33} value. The value of 190 pC/N is comparable to the highest values reported for the NKN–LT system. Although MnO modifications reduced dielectric losses, they also shifted the phase transition to a lower temperature. It is assumed that this transition occurs well-below the measurement temperature in these samples and the effects of the transition on d_{33} are less apparent. For this reason, d_{33} values decreased from 190 pC/N in undoped ceramics to $\sim$ 144 pC/N and 135 pC/N for the 0.5 and 1 mol% MnO samples respectively.

CONCLUSIONS

The introduction of MnO affected the structural and electrical properties of $Na_{0.465}K_{0.465}Li_{0.07}Nb_{0.93}Ta_{0.07}O_3$ ceramics, sintered at 1025 °C. Significant changes in peak intensity ratios in XRD patterns, were evidence that Mn^{2+}/Mn^{3+} ions were substituting on the perovskite lattice. The additive increased the amount of tetragonal polymorph co-existing with orthorhombic phase. Microstructures showed evidence of secondary recrystallization, the MnO modified samples were more uniform in grain size, consistent with a more advanced level of secondary grain growth. The Curie temperature increased from 396 °C to $\sim$ 420–435 °C, but the peak dielectric constant showed a 3-fold decrease in the MnO doped samples. The unmodified NKLNT samples gave a d_{33} value of 190 pC/N decreasing to $\sim$ 135 pC/N in the MnO doped ceramics. The higher room-temperature d_{33} value in the undoped samples is attributed to the beneficial effects of a orthorhombic-tetragonal polymorphic phase transition, with a peak temperature just above the measurement temperature.

ACKNOWLEDGMENTS

This work was financially supported by the Thailand Research Fund and Commission on Higher Education. The project was partly sponsored by the NANOTEC Centre of Excellence at Prince of Songkla University, Thailand.

REFERENCES

1. Jaffe B, Cook WR, Jaffe H (1971) *Piezoelectric Ceramics*, Academic Press, New York, p 92.
2. Moulson AJ, Herbert JM (1990) *Electroceramics – Materials, Properties, Applications*, Chapman & Hall, London.
3. Yimnirun R, Ananta S, Laoratakul P (2004) Dielectric properties of ceramics in lead zirconate titanate – lead magnesium niobate system. *Songklanakarin J Sci Tech* **26**, 529–36.
4. Birol H, Damjanovic D, Setter N (2006) Preparation and characterization of $(K_{0.5}Na_{0.5})NbO_3$ ceramics. *J Eur Ceram Soc* **26**, 861–6.
5. Guo Y, Kakimoto K-I, Ohsato H (2004) Dielectric and Piezoelectric Properties of Lead-Free $(Na_{0.5}K_{0.5})NbO_3$–$SrTiO_3$ Ceramics. *Solid State Comm* **129**, 279–84.
6. Zuo R, Rödel J, Chen R, Li L (2006) Sintering and electrical properties of lead-free $Na_{0.5}K_{0.5}NbO_3$ piezoelectric ceramics. *J Am Ceram Soc* **89**, 2010–5.
7. Saito Y, Takao H, Tani T, Nonoyama T, Takatori K, Homma T, Nagaya T, Nakamura M (2004) Lead-free piezoceramics. *Nature* **432**, 84–7.

8. Ahn C-W, Choi C-H, Park H-Y, Nahm S, Priya S (2008) Dielectric and piezoelectric properties of $(1-x)\,(Na_{0.5}K_{0.5})NbO_3$–$x\,BaTiO_3$ ceramics. *J Mater Sci* **43**, 6784–97.
9. Guo Y, Kakimoto K-I, Ohsato H (2004) Phase transitional behavior and piezoelectric properties of $(Na_{0.5}K_{0.5})NbO_3$–$LiNbO_3$ ceramics. *Appl Phys Lett* **85**, 4121–3.
10. Zhang S, Xia R, Shrout TR, Zang G, Wang J (2006) Piezoelectric properties in perovskite $0.948\,(K_{0.5}Na_{0.5})NbO_3$–$0.05\,LiSbO_3$ lead-free ceramics. *J Appl Phys* **100**, 104108.
11. Guo Y, Kakimoto K, Ohsato H (2005) $(Na_{0.5}K_{0.5})NbO_3$–$LiTaO_3$ lead-free piezoelectric ceramics. *Mater Lett* **59**, 241–4.
12. Saito Y, Takao H (2006) High performance lead-free piezoelectric ceramics in the (K,Na)NbO_3–$LiTaO_3$ solid solution system. *Ferroelectrics* **338**, 17–32.
13. Bomlai P, Sukprasert S, Muensit S, Milne SJ (2008) Reaction-sintering of lead-free piezoceramic compositions: $(0.95-x)\,Na_{0.5}\,K_{0.5}\,NbO_3$–$0.05\,LiTaO_3$–$x\,LiSbO_3$. *J Mater Sci* **43**, 6116–21.
14. Matsubara M, Kikuta KSH (2005) Piezoelectric properties of $(K_{0.5}Na_{0.5})\,(Nb_{1-x}Ta_x)O_3$–$K_{5.4}\,Cu\,Ta_{10}O_{29}$ ceramics. *J Appl Phys* **97**, 114105.
15. Chen R, Li L (2006) Sintering and electrical properties of lead-free $Na_{0.5}K_{0.5}NbO_3$ piezoelectric ceramics. *J Am Ceram Soc* **89**, 2010–5.
16. Du H, Liu D, Tang F, Zhu D, Wancheng Z (2007) Microstructure, piezoelectric, and ferroelectric properties of Bi_2O_3-added $(K_{0.5}Na_{0.5})NbO_3$ lead-free ceramics. *J Am Ceram Soc* **90**, 2824–9.
17. Skidmore TA, Comyn TP, Milne SJ (2009) Temperature stability of $([Na_{0.5}K_{0.5}NbO_3]_{0.93}$–$[LiTaO_3]_{0.07})$ lead-free piezoelectric ceramics. *Appl Phys Lett* **94**, 222902.
18. Hao J, Xu Z, Chu R, Zhang Y, Li G, Yin Q (2009) Effects of MnO_2 on phase structure, microstructure and electrical properties of $(K_{0.5}Na_{0.5})_{0.94}Li_{0.06}NbO_3$ lead-free ceramics. *Mater Chem Phys* **118**, 229–33.
19. Lin D, Kwok KW, Tian H, Chan HWL (2007) Phase transitions and electrical properties of $(Na_{1-x}K_x)(Nb_{1-y}Sb_y)O_3$ lead-free piezoelectric ceramics with a MnO_2 sintering aid. *J Am Ceram Soc* **90**, 1458–62.
20. Bomlai P, Sinsap P, Muensit S, Milne SJ (2008) Effect of MnO on the phase development, microstructures, and dielectric properties of $0.95\,Na_{0.5}K_{0.5}NbO_3$–$0.05\,LiTaO_3$ ceramics. *J Am Ceram Soc* **91**, 624–7.
21. Zuo R, Fu J, Su S, Fang X, Cao JL (2009) Electrical properties of manganese modified sodium potassium lithium niobate lead-free piezoelectric ceramics. *J Mater Sci Mater Electron* **20**, 212–6.
22. Skidmore TA, Milne SJ (2007) Phase development during mixed-oxide processing of a $[Na_{0.5}K_{0.5}NbO_3]_{1-x}$–$[LiTaO_3]_x$ powder. *J Mater Res* **22**, 2265–72.
23. ICDD (2001) Powder Diffraction File No. 32-0822, International Centre for Diffraction Data, Newton Squre, PA.
24. ICDD (2001) Powder Diffraction File No. 71-0945, International Centre for Diffraction Data, Newton Squre, PA.